

CHARACTERIZATION OF
FORMULATIONS

6.1 Introduction

Characterization of the developed formulation is required to have assurance that the product passes the desired quality attributes. Various characterization parameters like spherulite's size and zeta potential, morphology by Scanning electron microscopy (SEM) and Transmission electron microscopy (TEM), *in vitro* drug release (to study the drug release pattern and kinetics), % entrapment efficiency (% EE) and % drug loading, osmolality and electrolyte induced flocculation study were performed in present investigation. Gemcitabine Hydrochloride (GCH) loaded Non-PEGylated and PEGylated spherulites and similarly, Vinorelbine Tartrate (VLB) loaded Non-PEGylated and PEGylated spherulites were characterized.

6.2 Materials and Equipment

6.2.1 Materials

Gemcitabine HCl (GCH) was obtained as a gift sample from Sun Pharmaceutical Industries Ltd., Vadodara, India. Vinorelbine tartrate (VLB) was obtained as a gift sample from Cipla Ltd. Mumbai, India. Cholesterol (Chol), Mannitol, Potassium oleate and Triton X100 were purchased from Sigma Aldrich (St. Louis, MO, USA). Soyabean Phosphatidylcholine (SPC) 95% (PhospholiponVR 90 G) and 1,2-distearoyl-sn-glycero-3-phosphoethanolamine-N-[amino (polyethylene glycol)-2000] (DSPE-PEG 2000) were obtained as gift sample from Lipoid GmbH (Ludwigshafen, Germany). Dichloromethane, Methanol and Chloroform (A. R. grade) were purchased from S.D. Fine-chemicals limited (Vadodara, India). Distilled water was prepared using in-house distillation assembly. 0.22 μ membrane filter was purchased from Pall Life Sciences (Mumbai, India). All other reagents were purchased from S.D. Fine-chemicals limited, Baroda, India and were of analytical reagent grade.

6.2.2 Equipments

- Analytical Weighing Balance (ATX 224, Shimadzu, Japan)
- Vortex Mixer (Spinix-Vortex Shaker, Tarsons, India)
- Rotary evaporator (IKA RV10, Karnataka, India)
- Particle Size Analyzer 3000 HS (Zeta Sizer Nano Series, Malvern Instruments, UK)
- UV-Visible spectrophotometer (UV-1800, Shimadzu, Japan)
- Cooling Centrifuge (Remi Equipment, Mumbai, India)
- Nikon H600L Microscope (Nikon, Japan)
- Transmission Electron Microscope Tecnai 20 (Philips, Holland)
- Scanning Electron Microscope XL 30 ESEM (Philips, Netherlands)

- 3250 Single-Sample Osmometer (Advanced Instruments, Norwood, Massachusetts, USA)

6.3 Methods

6.3.1 Spherulites size and Zeta (ζ) potential

Briefly, 50 μ L of dispersion was diluted with 2 ml of distilled water and taken in disposable polystyrene cuvette. Mean hydrodynamic diameter, poly-dispersity index (PDI) and surface charge (ζ -potential) were measured in triplicate by dynamic light scattering using Malvern size analyzer (Malvern Nanoseries-ZS, Malvern Instruments, United Kingdom).

6.3.2 % Entrapment efficiency (% EE) and % Drug loading (% w/w)

Non-PEGylated and PEGylated spherulites loaded with GCH and VLB separately, were taken in different centrifuge tubes and centrifuged at 20000 RPM at 4 °C for 30 minutes (REMI Laboratory Instruments, Mumbai, India). Spherulites pellet settled at the bottom of tube was air dried and weighed for accounting the total weight of solid content. 2% Triton X100 solution was used to lyse the pellet and diluted suitably with distilled water. The amount of drug was estimated using UV-Vis spectrophotometer (Shimadzu 1800, Kyoto, Japan) at 266 nm for GCH and 271 nm for VLB. Supernatant was also diluted suitably and free drug amount was estimated to establish the mass balance.

Calculation of the % Entrapment Efficiency (EE) and loading (% w/w), was performed using following formulae:

$$\% EE = \frac{\text{Estimated Entrapped drug in Spherulites}}{\text{Total drug added during formulation}} \times 100 \dots \dots \dots (1)$$

$$\% \text{Drug Loading} \left(\% \frac{w}{w} \right) = \frac{\text{Estimated Entrapped drug in Spherulites}}{\text{Total weight of Spherulites after drying}} \times 100 \dots \dots (2)$$

6.3.3 Morphological analysis by SEM and TEM

6.3.3.1 SEM analysis

Morphological characteristics i.e. shape and surface properties of all the spherulites formulation was studied by using SEM micrographs. Prior SEM analysis, sample preparation was carried out. Briefly, a drop of dispersion was placed on one side of adhesive stub. The dispersion was allowed to air dry. Subsequently the stub was placed in the SEM instrument and examined photographically by a scanning electron microscope (XL 30 ESEM; Philips, Netherlands). Suitable magnification in the range of 7,500-20,000 X was used while taking

the photomicrographs.

6.3.3.2 TEM analysis

Morphology and internal structure of non-PEGylated and PEGylated spherulites (loaded separately with GCH and VLB) were observed by transmission electron microscopy (TEM) operated at 200 KV (Tecnai 20; Philips, Amsterdam, The Netherlands) with magnification power up to 75,000 X. Sample was prepared by adding a drop of the formulation on the carbon-coated copper grid and allowed to rest for one minute. Resting for a minute facilitates the spherulites to adhere onto carbon substrate. Excess formulation was blotted using a filter paper. A drop of 1 % Uranyl acetate solution was applied onto the grid for a minute and then allowed to be air dried. Grid was mounted on single tilt holder and inserted into the TEM instrument.

6.3.4 *In Vitro* drug release study

Optimized formulations i.e. Non-PEGylated and PEGylated formulation (separately loaded with GCH and VLB) along with standard drug solution were assessed for their drug release patterns and its kinetics. Briefly, Activated dialysis bag [1] (12K molecular weight cut off; Himedia, Mumbai, India) was used to fill, separately, 2 ml dispersion (containing 0.5 mg of GCH and VLB) of non-PEGylated spherulites, PEGylated spherulites and standard drug solution to study the *in vitro* drug release. Closure clips (Sigma Aldrich, Bengaluru, India) were used to seal both ends of dialysis bag, which was then suspended in 100 mL of PBS pH 7.4, taken as diffusion medium in a glass beaker. Diffusion medium maintained at 37 °C, was constantly stirred using a magnetic stirrer at 100 RPM. Aliquots of 5 mL were withdrawn at predetermined time interval (0, 1, 2, 4, 8, 12, 24, 36, 48 h) and the amount of drug in sample was estimated at 266 nm for GCH and 271 nm for VLB by UV spectrophotometer (Shimadzu 1800, Kyoto, Japan). Fresh diffusion medium was replenished at each time interval.

Various mathematical models were applied onto the results obtained from drug release study to assess the kinetics of release from formulation.

6.3.5 Determination of Osmolality

Non-PEGylated and PEGylated formulation separately loaded with GCH and VLB were evaluated for their osmolality. 0.2 ml of dispersion was taken in sample holding tube and kept in the freezing chamber of the osmometer (3250 Single-Sample Osmometer, Advanced Instruments, Norwood, Massachusetts, USA). Upon freezing the sample in the chamber, instrument displays the osmolality of the formulation.

6.3.6 Electrolyte-induced flocculation study

Electrolyte-induced flocculation study was performed to evaluate steric stability of spherulites. 0.2, 0.4, 0.8, 1.2, 1.6 and 2.0 M Sodium sulfate (Na_2SO_4) solution was prepared in 16.7%w/v sucrose solution. 1mg/ml lipid concentration of Non-PEGylated and PEGylated spherulites dispersion, separately loaded with GCH and VLB was mixed and volume was made up to 5 ml with previously prepared solution. The resulting dispersions were mixed and absorbance was measured within 5 minutes using UV spectrophotometer (Shimadzu 1800, Kyoto, Japan) at 400 nm [2]. Results were compared with diluted spherulites dispersion having 1 mg/ml lipid concentration.

6.4 Results and Discussion

6.4.1 GCH loaded Non-PEGylated and PEGylated Spherulites

6.4.1.1 Spherulites size and Zeta (ζ) potential

Vesicle size for both PEGylated as well as non PEGylated formulation has been reported in Table 6.1. Figure 6.1 and 6.2 shows the size distribution graphs. Results confirm that size was satisfactory for lung targeting and assure for EPR effect at tumor site while PDI of formulation indicate uniformity in size of vesicles (monosize). The ideal size range of spherulites were needed in the range of 100-750 nm for efficient lung targeting [3]. The zeta potential governs the physical stability of Spherulites. Zeta potential of the formulation (Figure 6.3 and 6.4) depends on the nature of lipid (natural or synthetic) with its molar concentration. It indicates the degree of repulsion between similarly charged particles in the formulation; this repulsive force prevents the particle aggregation during storage. It is known that, absolute Zeta potential value of above 30 mV is the indicator of good stability, by keeping and maintaining uniform dispersion of Spherulites. Zeta potential results as seen in Table 6.1 indicate that both the formulations are expected to have physical stability. Addition of PEG to the formulation further increases the negativity of zeta potential imparting more stability to the formulation. The increase in the zeta potential in negative direction can be due to two main reasons: The slipping of vesicular surface moved further away and reduces the zeta potential and also, the PEG chains present on the surface of the vesicles minimize the movements of the spherulites affecting the zeta potential to shift towards negative value [4].

Table 6.1: Results of size and zeta potential for GCH loaded Non-PEGylated and GCH loaded PEGylated Spherulites. Data represents mean of three experimental values (n=3; mean±SD).

	Size (PDI)	Zeta (ζ) Potential
GCH loaded Non-PEGylated Spherulites	204.9±1.2 nm (0.43±0.01)	-26.5±1.3 mV
GCH loaded PEGylated Spherulites	209.2±1.4 nm (0.43±0.03)	-33.3±1.6 mV

Results

Z-Average (d.nm): 204.9	Peak 1: 204.9	% Intensity: 83.6	Width (d.nm): 142.6
Pdl: 0.436	Peak 2: 0.000	0.0	0.000
Intercept: 0.635	Peak 3: 0.000	0.0	0.000
Result quality: Good			

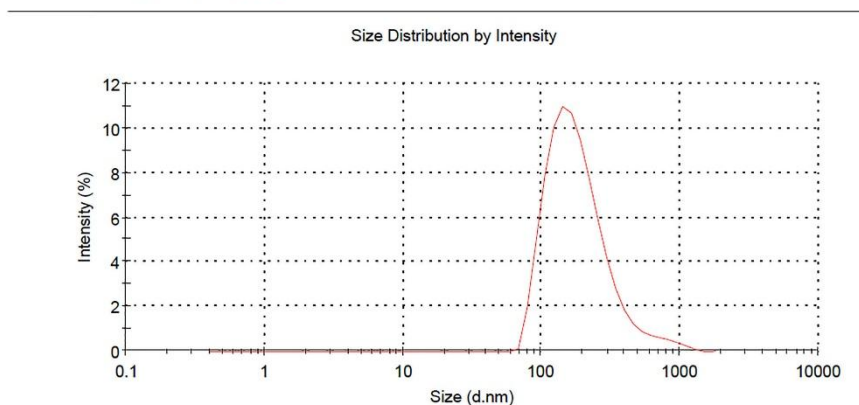


Figure 6.1: GCH loaded Non-PEGylated Spherulites size analysis.

Results

Z-Average (d.nm): 209.2	Peak 1: 209.2	% Intensity: 84.9	Width (d.nm): 145.1
Pdl: 0.436	Peak 2: 0.000	0.0	0.000
Intercept: 0.573	Peak 3: 0.000	0.0	0.000
Result quality: Good			

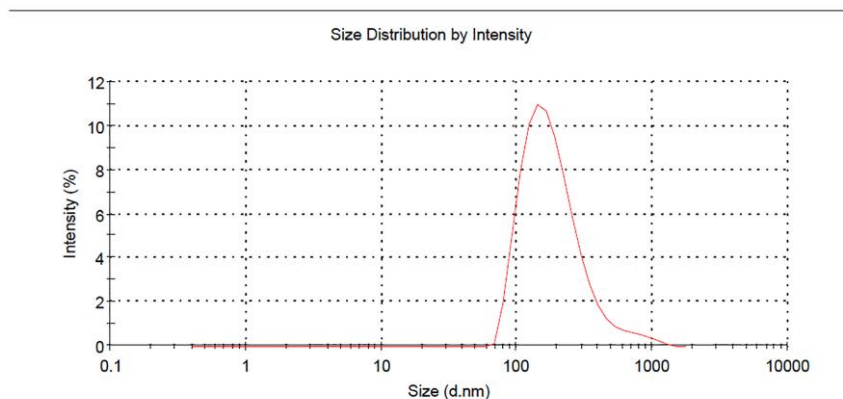
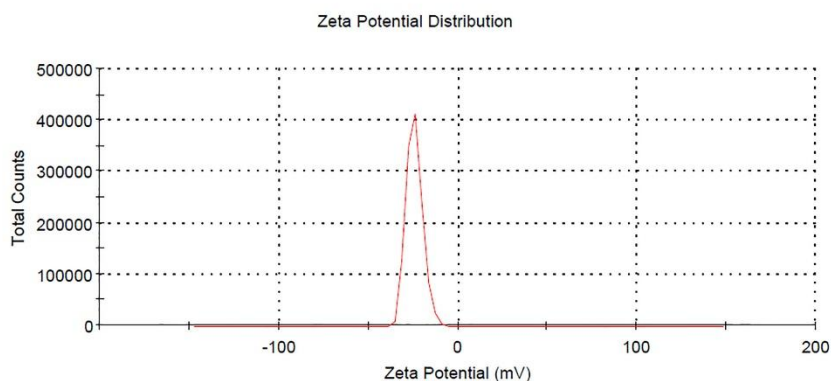


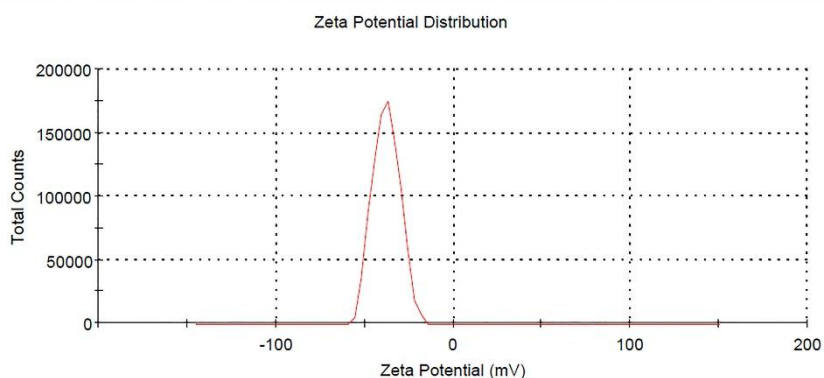
Figure 6.2: GCH loaded PEGylated Spherulites size analysis.

Results

	Mean (mV)	Area (%)	Width (mV)
Zeta Potential (mV): -26.5	Peak 1: -26.5	100.0	4.55
Zeta Deviation (mV): 4.55	Peak 2: 0.00	0.0	0.00
Conductivity (mS/cm): 0.00371	Peak 3: 0.00	0.0	0.00
Result quality Good			

**Figure 6.3:** GCH loaded Non-PEGylated Spherulites zeta potential analysis.**Results**

	Mean (mV)	Area (%)	Width (mV)
Zeta Potential (mV): -33.3	Peak 1: -33.3	100.0	6.38
Zeta Deviation (mV): 6.38	Peak 2: 0.00	0.0	0.00
Conductivity (mS/cm): 0.0283	Peak 3: 0.00	0.0	0.00
Result quality Good			

**Figure 6.4:** GCH loaded PEGylated Spherulites zeta potential analysis.**6.4.1.2 % Entrapment efficiency (%EE) and % Drug loading (%w/w)**

Gemcitabine hydrochloride was entrapped in to the spherulites with the entrapment efficiency of 76.28% for non-PEGylated formulation, while for PEGylated the entrapment efficiency was 77.42%. While loading efficiency was found to be 9.07%w/w and 9.38%w/w for PEGylated and non-PEGylated spherulites, respectively. This high percentage of entrapment of hydrophilic drug may be attributed to the multilamellar nature of the vesicles where aqueous spaces are present between the membranes in addition to the spaces at the center of the vesicles. Another reason is the presence of non-leaky bilayers resulting from the addition

of Chol, which increases the viscosity of the microenvironment and rigidity of the bilayers. Chol decreases the fluidity of membranes above the phase transition temperature, with a corresponding reduction in permeability to aqueous solutes. Chol can be incorporated up to a level of 50 mol % i.e. SPC:Chol 1:1 molar ratio, at which it displays maximum stabilising effect both in vitro and in vivo. Spherulites thus displayed high entrapment of a hydrophilic drug candidate. PEG incorporation into vesicles did not affect the entrapment efficiency of the drug as seen from the results in Table 6.2. The hydrophilic PEG chains are able to increase the stability and circulation time of spherulites. PEG is an inert biodegradable excipients reduces the chances of any toxicity or bioaccumulation [4].

Table 6.2: Results of % EE and % drug loading (% w/w) for GCH loaded Non-PEGylated and GCH loaded PEGylated Spherulites. Data represents mean of three experimental values (n=3; mean±SD).

	% EE	% Drug loading (%w/w)
GCH loaded Non-PEGylated Spherulites	76.28±1.1	9.38±0.94
GCH loaded PEGylated Spherulites	77.42±1.5	9.07±0.89

6.4.1.3 Morphological analysis by SEM and TEM

SEM techniques works on the principle of striking the sample with accelerated primary electrons. Upon striking secondary electrons are produced, which are collected by a positive charged electron detector and gives a 3D image of the specimen [5]. SEM analysis was performed to study the surface morphology of both formulations i.e. GCH loaded Non-PEGylated and PEGylated spherulites.

SEM images of Non-PEGylated and PEGylated spherulites are shown in Figure 6.5 and 6.6, respectively. The micrographs revealed that the spherulites were discrete, uniformly spherical in shape with no signs of aggregation.



Figure 6.5: SEM image of GCH loaded Non-PEGylated Spherulites.

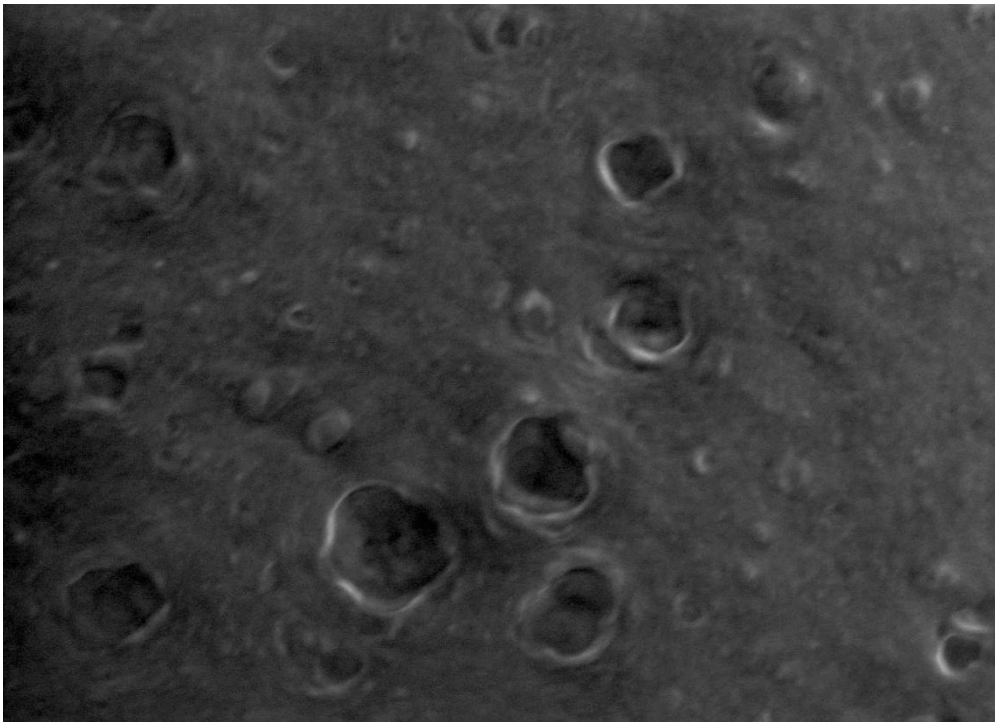


Figure 6.6: SEM image of GCH loaded PEGylated Spherulites.

Working principle of TEM is striking the sample with accelerated electrons. The transmitted electrons through sample are collected by an anode plate and an image is produced. Transmission electron microscopy images shown in Figure 6.7 and 6.8 for Non-PEGylated and PEGylated spherulites, respectively, demonstrate the formation of vesicles with multiple

lamellas. Figure 6.8 which represents PEGylated Spherulites shows a dark rim around the vesicle caused by greater projection of electron beam due to PEG chains attached to the vesicle surface. PEG layer appears electron opaque giving a dark appearance on the image. This dark contour derives from the scattering of electrons in the part of beam that encounters the PEG layer surrounding the spherulites surface [6-9]. The vesicles were spherical and did not show any agglomeration. The results were in agreement with the size obtained by Malvern size analyser (Malvern Nanoseries-ZS, Malvern Instruments, Malvern, UK) [4].

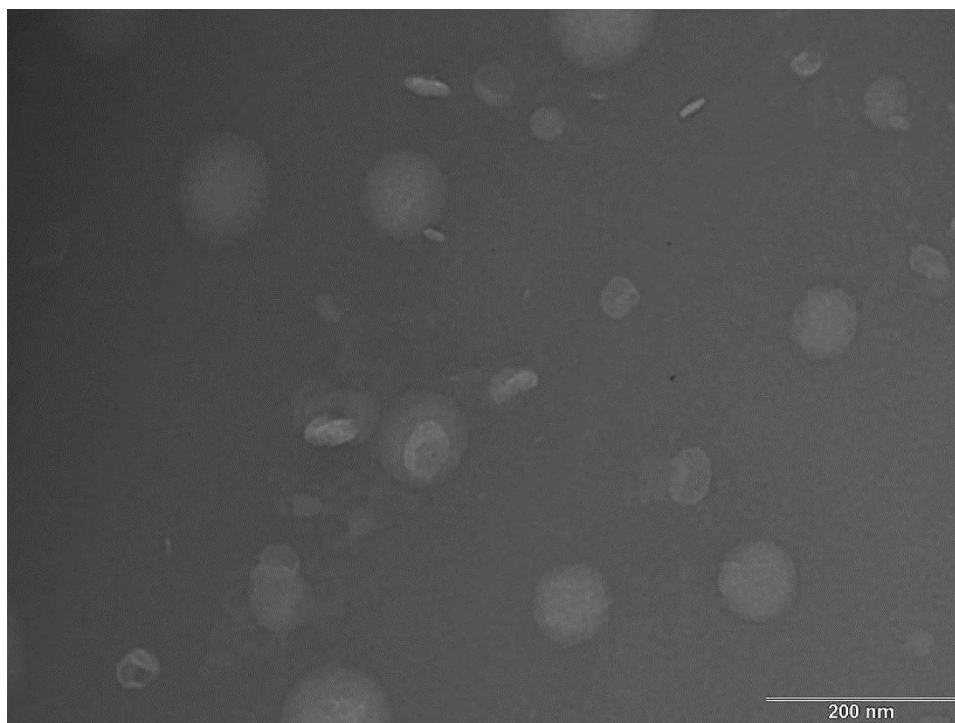


Figure 6.7: TEM image of GCH loaded Non-PEGylated Spherulites.

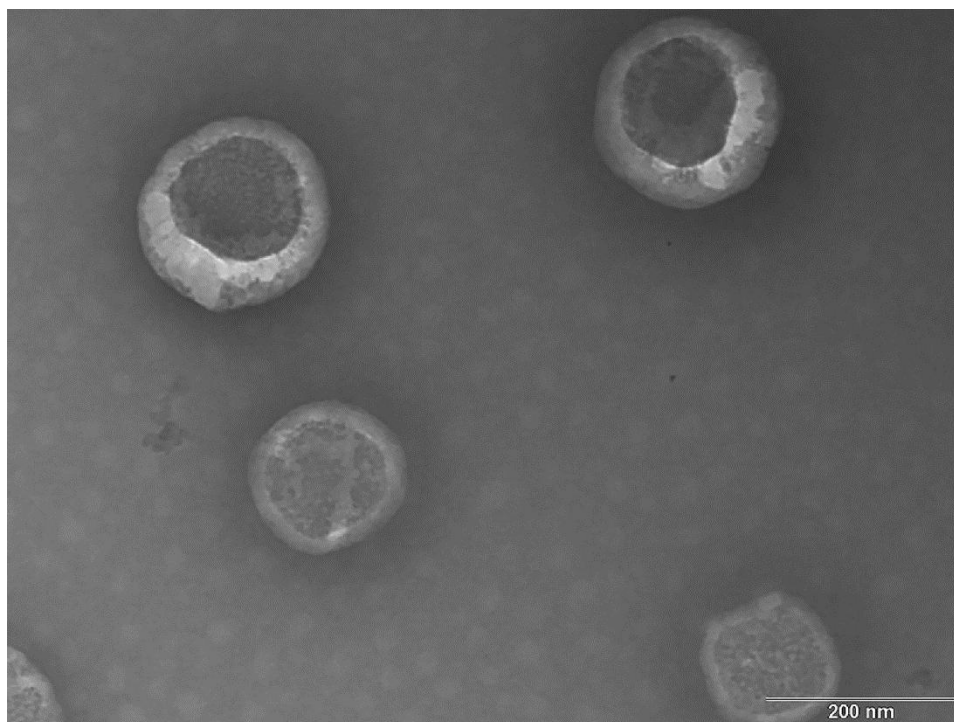


Figure 6.8: TEM image of GCH loaded PEGylated Spherulites.

6.4.1.4 *In Vitro* drug release study

The results of the *in vitro* drug release studies are shown in Table 6.3 and Figure 6.9. Standard GCH solution showed 78.76% release after 1 h and within 2 h entire drug was diffused through the dialysis bag. This was followed by non-PEGylated, which showed 93.09% drug release and PEGylated spherulites 89.49% after 48 h as seen in Figure 6.9. PEGylation of spherulites relatively retarded the drug release compared to non-PEGylated formulation, however the difference was found to be statistically insignificant ($p=0.85$ at 95% confidence interval (CI)). PEG serves as a barrier for release of hydrophilic drug from spherulites. Moreover, PEGylation of spherulites can enable the formulation to remain in the circulation for extended period of time. The kinetics of drug release was evaluated by fitting the release data in various mathematical model. First order model fitted the best with highest R^2 value. Release from vesicular system is generally first order i.e. dependent on the concentration of drug in spherulites. This kinetics gives rise to high initial drug concentrations followed by progressively lower levels for longer period of time. First order release is a linear kinetic process, where, rate of drug release increases with the drug concentration [4].

Table 6.3: *In Vitro* drug release study of Standard GCH solution, GCH loaded Non-PEGylated Spherulites and GCH loaded PEGylated Spherulites. Data represents mean of three experimental values (n=3; mean±SD).

Time (Hrs)	% Cumulative drug release		
	Standard GCH solution	GCH loaded Non-PEGylated Spherulites	GCH loaded PEGylated Spherulites
0	0±0	0±0	0±0
1	78.76±2.0	15.56±1.87	17.90±1.13
2	98.54±1.89	18.68±1.20	24.51±1.36
4		25.10±1.40	34.82±1.89
8		35.41±2.10	46.89±1.49
12		58.85±1.96	64.59±0.97
24		77.53±1.37	73.74±1.24
36		85.41±1.69	83.07±1.48
48		93.09±1.21	89.49±1.65

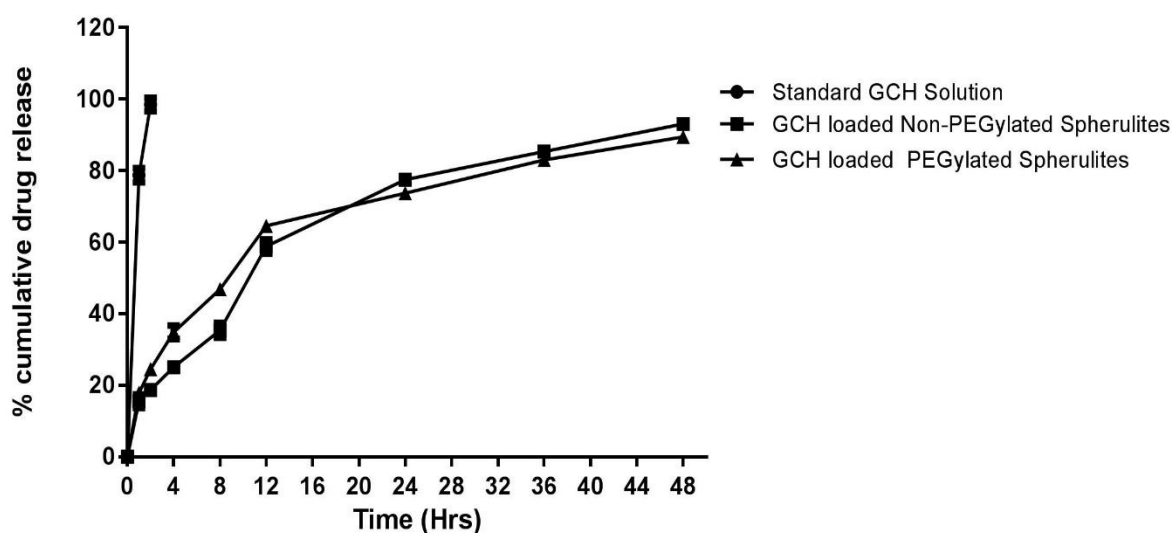


Figure 6.9: *In Vitro* drug release study of Standard GCH solution, GCH loaded Non-PEGylated Spherulites and GCH loaded PEGylated Spherulites. Data represents mean of three experimental values (n=3; mean±SD).

6.4.1.5 Determination of Osmolality

Biological membranes are sensitive to osmotic gradients of the formulation. It is recommended by regulatory authorities to monitor the osmolality of a newly developed formulation [10]. Osmotic gradient of a formulation plays a pivotal role in membrane fusion-dependent processes such as cellular uptake. It is also reported that unilamellar vesicles tend to lyse prematurely due to osmotic stress. Whereas, multilamellar vesicles like spherulites have the advantage of onion like internal structure, which protects the encapsulated drug from premature release [11]. Osmolality of GCH loaded Non-PEGylated Spherulites and GCH loaded PEGylated Spherulites was measured using 3250 Single-Sample Osmometer (Advanced Instruments, Norwood, Massachusetts, USA). The instrument works on the principle of freezing point depression, which is a colligative property, where, the freezing point gets lowered as the solute concentration increases in the solvent. Reference range of osmolality is 275–295 mOsm/kg [12].

Results of osmolality for GCH loaded Non-PEGylated Spherulites and GCH loaded PEGylated Spherulites are given in Table 6.4.

Table 6.4: Results of osmolality determination of GCH loaded Non-PEGylated Spherulites and GCH loaded PEGylated Spherulites. Data represents mean of three experimental values (n=3; mean±SD).

	Osmolality (mOsm/Kg)
GCH loaded Non-PEGylated Spherulites	282±1.2
GCH loaded PEGylated Spherulites	291±1.4

6.4.1.6 Electrolyte-induced flocculation study

Flocculation stability of GCH loaded Non-PEGylated and PEGylated spherulites was assessed by increasing the sodium sulfate concentration, which was evidenced by changes observed in absorbance at 400 nm. Table 6.5 and Figure 6.10 depicts the results of electrolyte-induced flocculation study. 1 mg/ml Non-PEGylated and PEGylated spherulites formulation dispersed in distilled water separately was used as control. Results showed that the absorbance remained unchanged till 1.2 M Na₂SO₄. However, as the concentration went on increasing the absorbance also up surged. This indicated that both the formulations i.e. Non-PEGylated and PEGylated spherulites were stable up to 1.2 M concentration of sodium sulfate. Steric barrier around the spherulites inhibited the flocculation induced by addition of an electrolyte. However, increase in electrolyte concentration above certain level disrupted the steric barrier and caused flocculation or aggregation of spherulites [2].

Table 6.5: Results of Electrolyte-induced flocculation study of GCH loaded Non-PEGylated Spherulites and GCH loaded PEGylated Spherulites. Data represents mean of three experimental values (n=3; mean±SD).

Na ₂ SO ₄ concentration (M)	GCH loaded Non-PEGylated Spherulites (absorbance at 400 nm)	GCH loaded PEGylated Spherulites (absorbance at 400 nm)
0	0.20±0.012	0.19±0.010
0.2	0.23±0.010	0.25±0.016
0.4	0.31±0.014	0.34±0.014
0.8	0.39±0.010	0.40±0.012
1.2	0.61±0.012	0.63±0.011
1.6	2.19±0.011	1.97±0.010
2.0	2.27±0.015	2.15±0.011

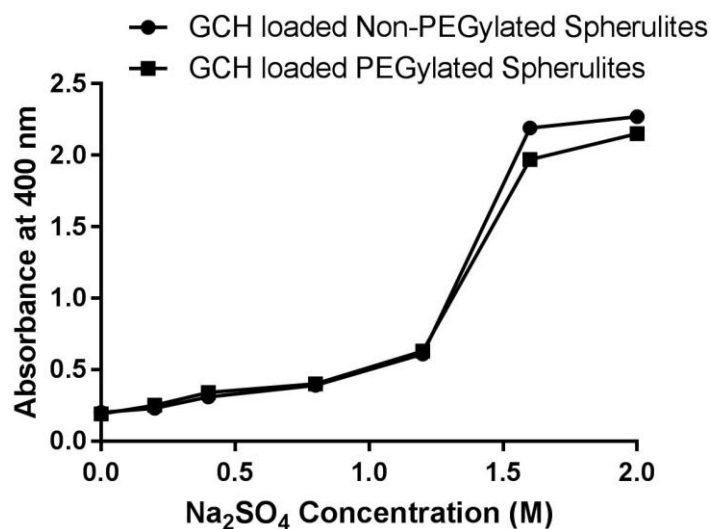


Figure 6.10: Graphical representation of Electrolyte-induced flocculation study of GCH loaded Non-PEGylated Spherulites and GCH loaded PEGylated Spherulites. Data represents mean of three experimental values (n=3; mean±SD).

6.4.2 VLB loaded Non-PEGylated and PEGylated Spherulites

6.4.2.1 Spherulites size and Zeta (ζ) potential

Both the formulations i.e. PEGylated and non PEGylated spherulites exhibited desired vesicular size as shown in Table 6.6. Figure 6.11 and 6.12 shows the size distribution graphs. The low PDI of the formulations indicated uniformity of size distribution (monodispersed).

The lower size of formulations is expected to target the drug to the lungs via the EPR effect. Zeta potential indicates the physical stability of Spherulites. Charge present on the surface plane of vesicles demonstrates whether there will be a repulsion or aggregation between the dispersed particles. The colloidal dispersion shows stability when particles bear identical charges; this force prevent aggregation or coagulation of the particles during their shelf life. Zeta potential of a vesicular system is majorly dominated by the nature and molar concentration of lipid (natural or synthetic). -30 mV zeta potential value indicates good stability, making it evenly distributed. As it is an established fact that higher the absolute value of zeta potential more the stability of a colloidal dispersion. Results of zeta potential given in Table 6.6 along with figure 6.13 and 6.14, shows that both the formulations are expected to be stable. PEG incorporation in the formulation additionally impart negative zeta potential over the spherulites improving the stability. It can be explained by two main reasons: (i) vesicular surface further slips away and reduces the zeta potential and (ii) PEG chain network present on the surface of vesicles restrict the movement of spherulites [13].

Table 6.6: Results of size and zeta potential for VLB loaded Non-PEGylated and VLB loaded PEGylated Spherulites. Data represents mean of three experimental values ($n=3$; mean \pm SD).

	Size (PDI)	Zeta (ζ) Potential
VLB loaded Non-PEGylated Spherulites	122.4 \pm 1.6 nm (0.24 \pm 0.03)	-26.9 ± 2.4 mV
VLB loaded PEGylated Spherulites	131.6 \pm 1.9 nm (0.32 \pm 0.01)	-37.8 ± 2.1 mV

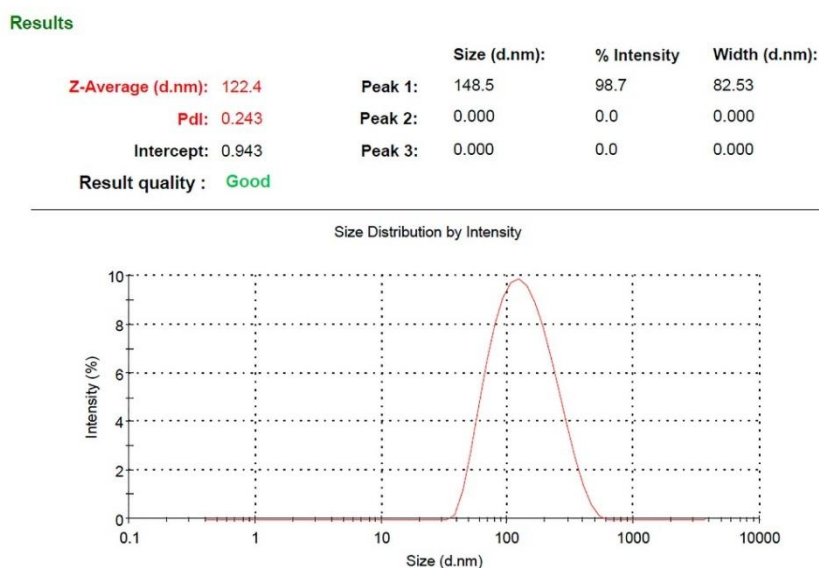


Figure 6.11: VLB loaded Non-PEGylated Spherulites size analysis.

Results

	Size (d.nm):	% Intensity	Width (d.nm):
Z-Average (d.nm): 131.6	Peak 1: 136.1	98.8	46.91
Pdl: 0.326	Peak 2: 0.000	0.0	0.000
Intercept: 0.912	Peak 3: 0.000	0.0	0.000
Result quality : Good			

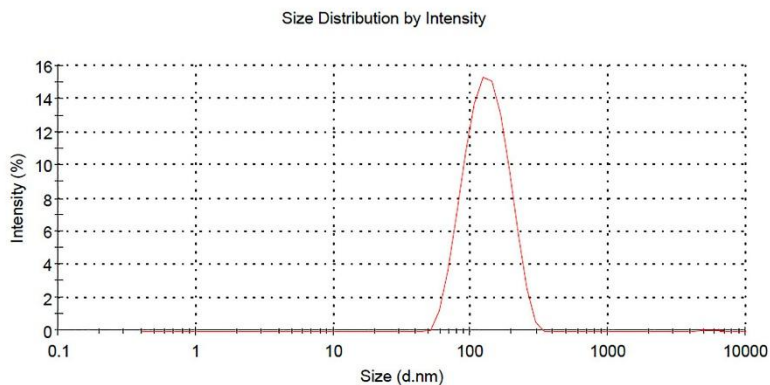


Figure 6.12: VLB loaded PEGylated Spherulites size analysis.

Results

	Mean (mV)	Area (%)	Width (mV)
Zeta Potential (mV): -26.9	Peak 1: -26.9	100.0	4.62
Zeta Deviation (mV): 4.62	Peak 2: 0.00	0.0	0.00
Conductivity (mS/cm): 0.00368	Peak 3: 0.00	0.0	0.00
Result quality Good			

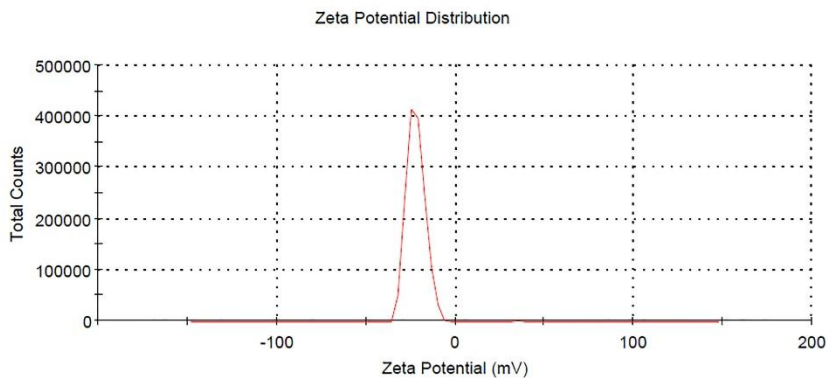


Figure 6.13: VLB loaded Non-PEGylated Spherulites zeta potential analysis.

Results

	Mean (mV)	Area (%)	Width (mV)
Zeta Potential (mV): -37.8	Peak 1: -37.8	100.0	5.32
Zeta Deviation (mV): 5.32	Peak 2: 0.00	0.0	0.00
Conductivity (mS/cm): 0.00706	Peak 3: 0.00	0.0	0.00
Result quality Good			

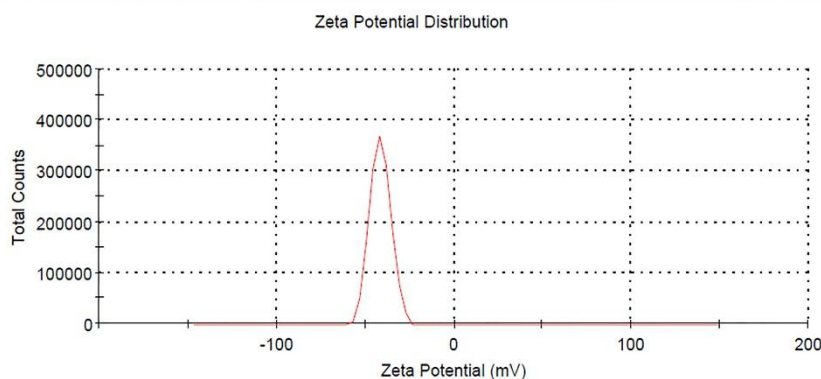


Figure 6.14: VLB loaded PEGylated Spherulites zeta potential analysis.

6.4.2.2 % Entrapment efficiency (%EE) and % Drug loading (%w/w)

VLB loaded non-PEGylated Spherulites exhibited 95.65% entrapment efficiency, whereas, PEGylated formulation gave 94.2%. While, drug loading for non-PEGylated and PEGylated spherulites was found to be 11.76 %w/w and 11.04 %w/w, respectively. High entrapment efficiency of hydrophilic drug candidate can be justified by presence of multiple lamellae in the vesicles. Aqueous spaces are present between the membranes or lamellae along with center space of the vesicle, which is, due to use of high concentration of amphiphilic lipid. Moreover, addition of cholesterol made the bilayers non-leaky by immobilizing the acyl chains of phospholipid and thereby enhancing their rigidity and viscosity of its microenvironment. Addition of cholesterol decreases the membrane fluidity above phase transition temperature, with a corresponding reduction of permeability to aqueous solutes. Cholesterol contributes actively to the stability of vesicles, as it is previously reported to use up to 50 mol % which becomes 1:1M ratio with lipid (i.e. SPC: Chol), showing maximum stabilizing effect in both in vitro and in vivo conditions. Results from Table 6.7 showed that there was no significant effect of the presence of PEG on drug entrapment efficiency and drug loading. Circulation time of spherulites significantly increases due to the hydrophilic PEG chains. Apparent decrease or slower leakage and increased stability of encapsulated drug can be explained by the presence of an envelope of PEG chains over spherulites surface [13].

Table 6.7: Results of % EE and % drug loading (% w/w) for VLB loaded Non-PEGylated and VLB loaded PEGylated Spherulites. Data represents mean of three experimental values (n=3; mean±SD).

	% EE	% Drug loading (%w/w)
VLB loaded Non-PEGylated Spherulites	95.65±0.86	11.76±0.59
VLB loaded PEGylated Spherulites	94.20±0.74	11.04±0.76

6.4.2.3 Morphological analysis by SEM and TEM

SEM analysis of VLB loaded Non-PEGylated spherulites and VLB loaded PEGylated spherulites was performed. SEM images shown in Figure 6.15 of Non-PEGylated spherulites and Figure 6.16 of PEGylated spherulites revealed that spherulites were discrete, uniformly spherical in shape with no signs of aggregation.

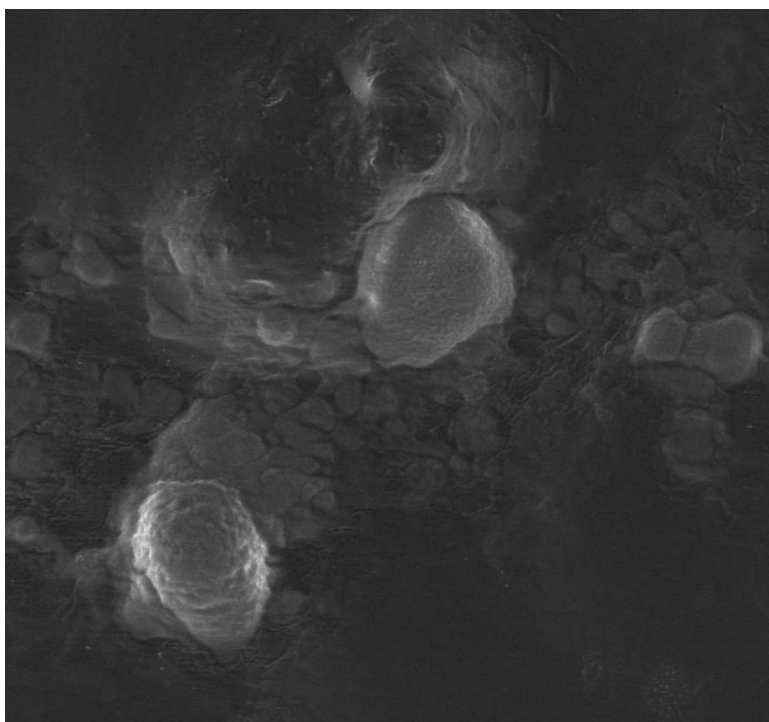


Figure 6.15: SEM image of VLB loaded Non-PEGylated Spherulites.

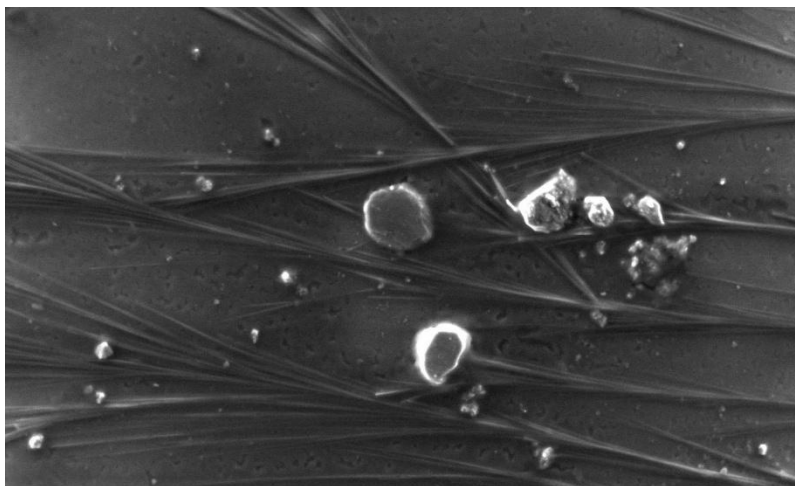


Figure 6.16: SEM image of VLB loaded PEGylated Spherulites.

TEM imaging was carried out to get more insight of internal architecture of vesicles. Non-PEGylated and PEGylated Spherulites micrographs shown in Figure 6.17 and 6.18 respectively. Images illustrate the Spherulites with multiple lamellas formed internally. Figure 6.8 which represents PEGylated Spherulites shows a dark rim around the vesicle caused by greater projection of electron beam due to PEG chains attached to the vesicle surface. PEG layer appears electron opaque giving a dark appearance on the image. This dark contour derives from the scattering of electrons in the part of beam that encounters the PEG layer surrounding the spherulites surface [6-9]. Vesicles were spherical in shape with no agglomeration seen. These results were in accordance with size analysis done by Malvern size analyzer (Malvern Nanoseries-ZS, Malvern Instruments, United Kingdom) [13].

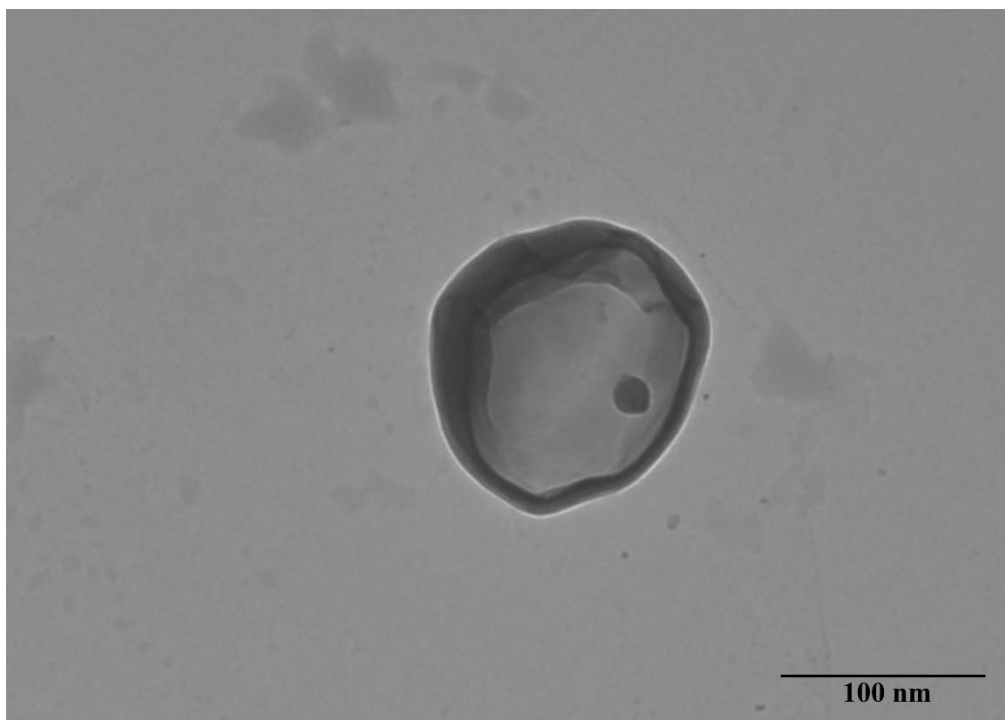


Figure 6.17: TEM image of VLB loaded Non-PEGylated Spherulites.

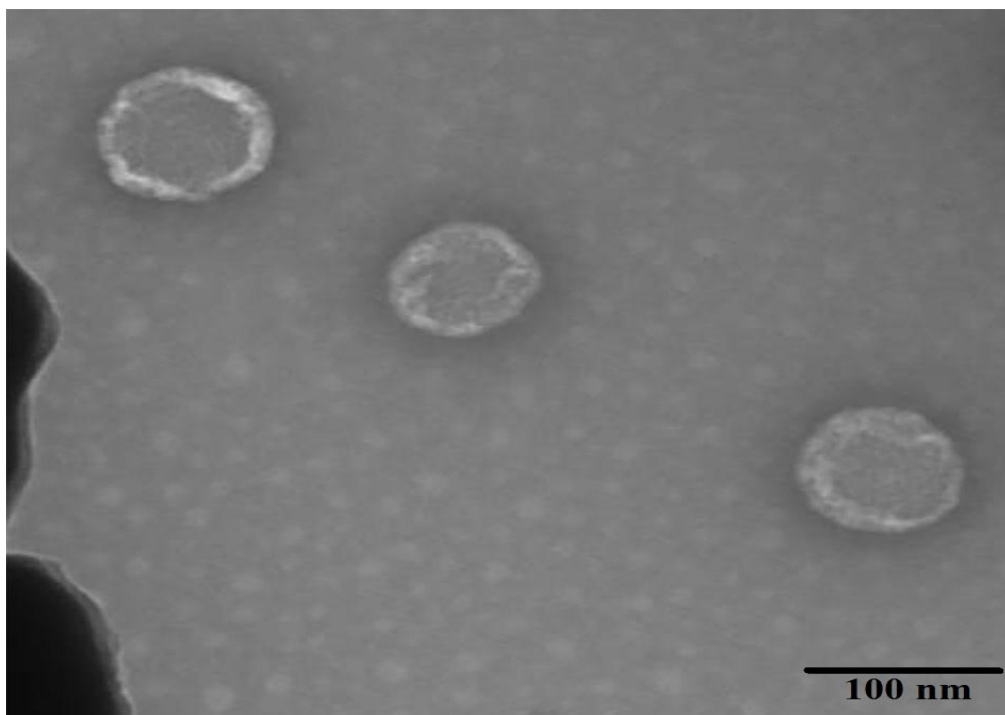


Figure 6.18: TEM image of VLB loaded PEGylated Spherulites.

6.4.2.4 *In Vitro* drug release study

The results of in vitro drug release study are shown in Table 6.8. VLB plain drug solution exhibited 92.3% release after 12 h and within 24 h entire drug got diffused through dialysis bag. Whereas, non-PEGylated Spherulites showed drug release of 90.84%, followed by PEGylated Spherulites 86.85% at the end of 48 h as seen in Figure 6.19. There was no

statistical significant difference between the release patterns of non-PEGylated and PEGylated spherulites ($p=0.99$ at 95% CI). PEGylation of spherulites can enable the formulation to remain in the circulation for extended period of time. Drug release kinetics was calculated by applying various mathematical models to release data. First order model showed best fit as it exhibited highest R^2 value. Generally, vesicles obey first order kinetics i.e. drug release is dependent on the concentration of drug encapsulated in spherulites. First order kinetics offers high drug concentration initially and followed by lower amount of drug for extended period of time [13].

Table 6.8: *In Vitro* drug release study of Standard VLB solution, VLB loaded Non-PEGylated Spherulites and VLB loaded PEGylated Spherulites. Data represents mean of three experimental values ($n=3$; mean \pm SD).

Time (Hrs)	% Cumulative drug release		
	Standard VLB solution	VLB loaded Non-PEGylated Spherulites	VLB loaded PEGylated Spherulites
0	0 \pm 0	0 \pm 0	0 \pm 0
1	25.39 \pm 0.76	10.86 \pm 0.67	11.85 \pm 1.38
2	39.78 \pm 1.12	25.70 \pm 0.86	23.71 \pm 1.78
4	50.11 \pm 1.51	32.57 \pm 1.43	34.56 \pm 1.86
8	74.89 \pm 1.43	43.43 \pm 1.56	46.41 \pm 0.98
12	92.30 \pm 1.13	57.27 \pm 1.47	59.26 \pm 1.28
24		73.11 \pm 1.31	72.11 \pm 1.56
36		81.97 \pm 1.25	80.98 \pm 1.47
48		90.84 \pm 1.45	86.85 \pm 1.20

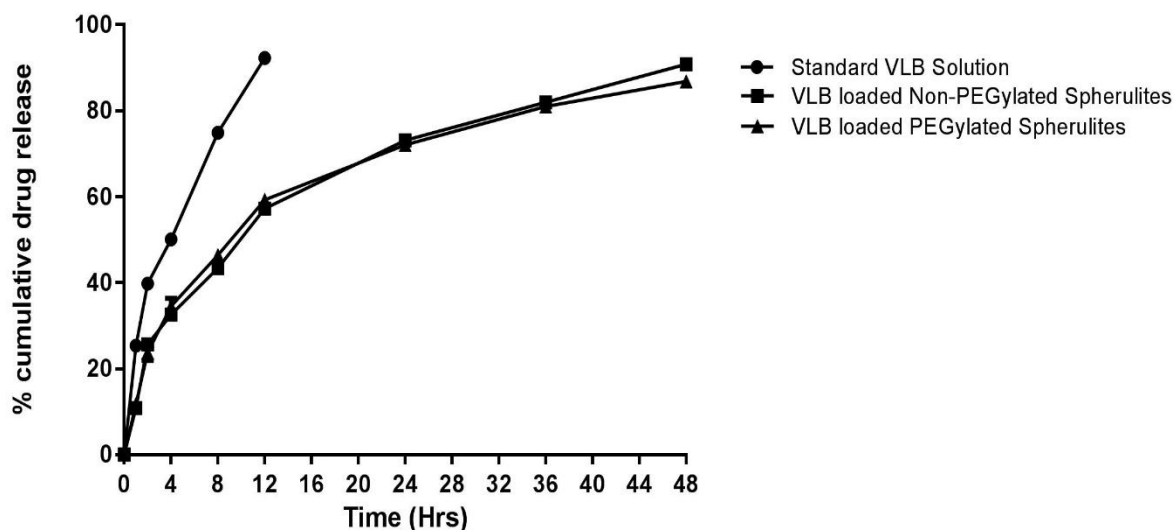


Figure 6.19: *In vitro* drug release study of Standard VLB solution, VLB loaded Non-PEGylated Spherulites and VLB loaded PEGylated Spherulites. Data represents mean of three experimental values (n=3; mean±SD).

6.4.2.5 Determination of Osmolality

The osmolality of VLB loaded Non-PEGylated Spherulites and VLB loaded PEGylated Spherulites was measured using 3250 Single-Sample Osmometer (Advanced Instruments, Norwood, Massachusetts, USA). Reference range of osmolality is 275–295 mOsm/kg [12]. Results of osmolality for GCH loaded Non-PEGylated Spherulites and GCH loaded PEGylated Spherulites are given in Table 6.9.

Table 6.9: Results of osmolality determination of VLB loaded Non-PEGylated Spherulites and VLB loaded PEGylated Spherulites. Data represents mean of three experimental values (n=3; mean±SD).

	Osmolality (mOsm/Kg)
VLB loaded Non-PEGylated Spherulites	284±1.4
VLB loaded PEGylated Spherulites	292±1.6

6.4.2.6 Electrolyte-induced flocculation study

Flocculation stability of VLB loaded Non-PEGylated and PEGylated spherulites was assessed by increasing the sodium sulfate concentration, which was evidenced by changes observed in absorbance at 400 nm. Table 6.10 and Figure 6.20 depicts the results of electrolyte-induced flocculation study. 1 mg/ml Non-PEGylated and PEGylated spherulites formulation dispersed in distilled water separately was used as control.

Results indicated that the absorbance was stable till 1.2 M Na_2SO_4 . However, further increase in concentration resulted in flocculation of spherulites in both the formulation which was evidenced by sudden increase in absorbance. Increase in electrolyte concentration disturbed the steric barrier of vesicles resulting into aggregation [2].

Table 6.10: Results of Electrolyte-induced flocculation study of VLB loaded Non-PEGylated Spherulites and VLB loaded PEGylated Spherulites. Data represents mean of three experimental values (n=3; mean±SD).

Na_2SO_4 concentration (M)	VLB loaded Non-PEGylated Spherulites (absorbance at 400 nm)	VLB loaded PEGylated Spherulites (absorbance at 400 nm)
0	0.19±0.010	0.20±0.012
0.2	0.21±0.011	0.23±0.014
0.4	0.33±0.012	0.36±0.015
0.8	0.36±0.011	0.39±0.012
1.2	0.59±0.010	0.55±0.014
1.6	2.27±0.013	2.05±0.011
2.0	2.41±0.012	2.36±0.014

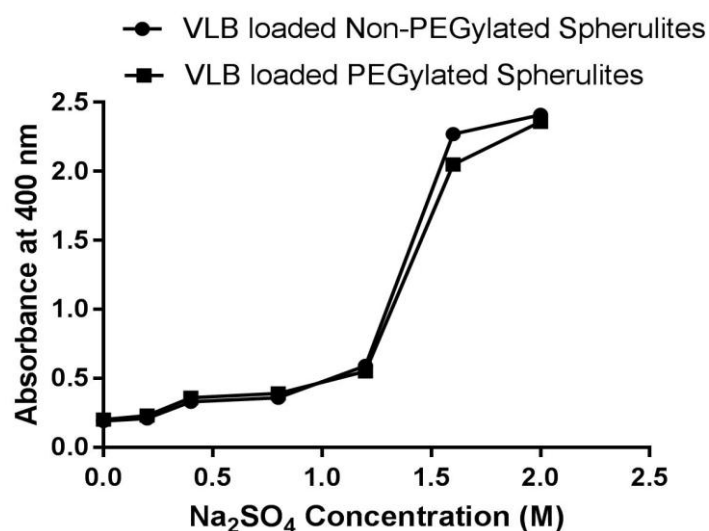


Figure 6.20: Graphical representation of Electrolyte-induced flocculation study of VLB loaded Non-PEGylated Spherulites and VLB loaded PEGylated Spherulites. Data represents mean of three experimental values (n=3; mean±SD).

6.5 References

1. Nounou, M., El-Khordagui, L. K., Khalafallah, N. A., & Khalil, S. A. (2006). In vitro drug release of hydrophilic and hydrophobic drug entities from liposomal dispersions and gels. *Acta Pharmaceutica*, 56(3), 311-324.
2. Subramanian, N., & Murthy, R. S. R. (2004). Use of electrolyte induced flocculation technique for an in vitro steric stability study of steric stabilized liposome formulations. *Die Pharmazie-An International Journal of Pharmaceutical Sciences*, 59(1), 74-76.
3. Dhand, C., Prabhakaran, M. P., Beuerman, R. W., Lakshminarayanan, R., Dwivedi, N., & Ramakrishna, S. (2014). Role of size of drug delivery carriers for pulmonary and intravenous administration with emphasis on cancer therapeutics and lung-targeted drug delivery. *RSC Advances*, 4(62), 32673-32689.
4. Dhande, R., Tyagi, A., Sharma, R. K., & Thakkar, H. (2017). Biodistribution study of ^{99m}Tc-gemcitabine-loaded spherulites in Sprague–Dawley rats by gamma scintigraphy to investigate its lung targeting potential. *Journal of microencapsulation*, 34(7), 623-634.
5. The History and Working Principle of the Scanning Electron Microscope (SEM). Available online: <https://www.azonano.com/article.aspx?ArticleID=3995>. (Accessed on March 14, 2018).
6. Zanetti-Ramos, B. G., Fritzen-Garcia, M. B., Creczynski-Pasa, T. B., Oliveira, C. S. D., Pasa, A. A., Soldi, V., & Borsali, R. (2010). Characterization of polymeric particles with electron microscopy, dynamic light scattering, and atomic force microscopy. *Particulate Science and Technology*, 28(5), 472-484.
7. Shay, J. S., English, R. J., Spontak, R. J., Balik, C. M., & Khan, S. A. (2000). Dispersion polymerization of polystyrene latex stabilized with novel grafted poly (ethylene glycol) macromers in 1-propanol/water. *Macromolecules*, 33(18), 6664-6671.
8. Rangelov, S., Momekova, D., & Almgren, M. (2010). Structural characterization of lipid-based colloidal dispersions using cryogenic transmission electron microscopy. *Microscopy: Science, Technology, Applications and Education*, 1724-1734.
9. Jung, H. T., Coldren, B., Zasadzinski, J. A., Iampietro, D. J., & Kaler, E. W. (2001). The origins of stability of spontaneous vesicles. *Proceedings of the National Academy of Sciences*, 98(4), 1353-1357.
10. Liposome Drug Products Chemistry, Manufacturing, and Controls; Human Pharmacokinetics and Bioavailability; and Labeling Documentation. U.S. Department of Health and Human Services Food and Drug Administration Center for Drug Evaluation

and Research (CDER). Available online <https://www.fda.gov/downloads/drugs/guidances/ucm070570.pdf>. (Accessed on March 14, 2018).

11. Mui, B. L., Cullis, P. R., Evans, E. A., & Madden, T. D. (1993). Osmotic properties of large unilamellar vesicles prepared by extrusion. *Biophysical journal*, 64(2), 443-453.
12. Serum Osmolality. Available online <https://emedicine.medscape.com/article/2099042-overview> (Accessed on 16th March 2018).
13. Dhande, R., Tyagi, A., Sharma, R. K., & Thakkar, H. (2018). ^{99m}Tc-vinorelbine tartrate loaded spherulites: Lung disposition study in Sprague-Dawley rats by gamma scintigraphy. *Pulmonary Pharmacology & Therapeutics* (10.1016/j.pupt.2018.01.002).